Electronic Supplementary Information (ESI)

4-Pentenoyl-isoleucyl-chitosan oligosaccharide and acrylamide functional monomers-dependent hybrid bilayer molecularly imprinted membrane for sensitive electrochemical sensing of bisphenol A

Qing Gao, Yang Zang*, Ju Xie, Yongchuan Wu, Huaiguo Xue*

School of Chemistry and Chemical Engineering, Yangzhou University, Yangzhou, Jiangsu, 225002, P. R. China

Corresponding authors

*E-mails: zangyang@yzu.edu.cn (Y. Zang), chhgxue@yzu.edu.cn (H. Xue).

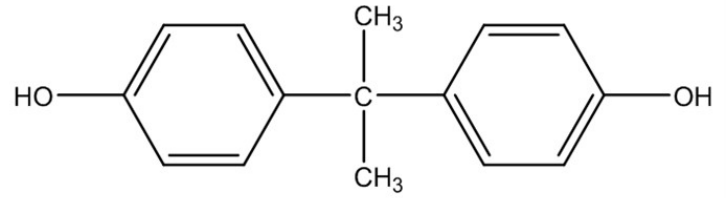

Scheme S1 Chemical structure of bisphenol A (BPA).

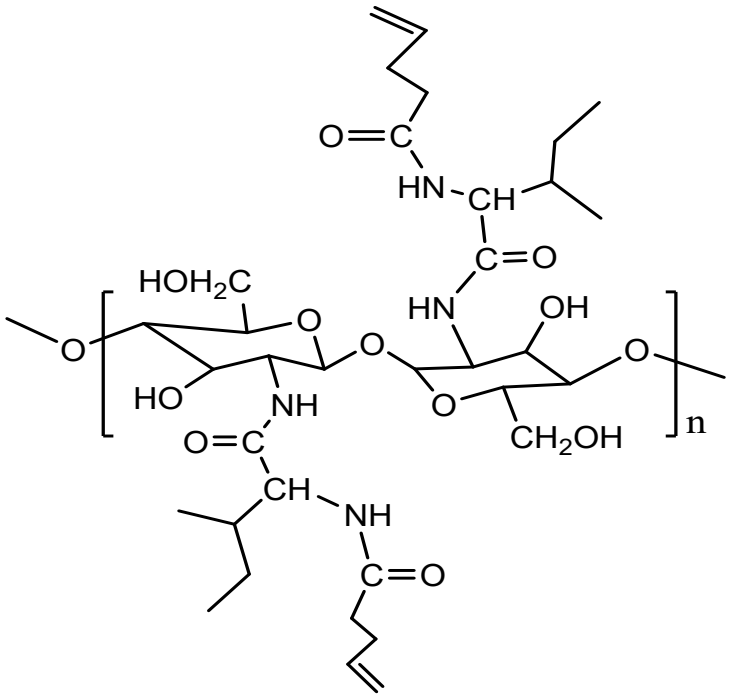

Scheme S2 Chemical structure of 4-pentenoyl-aminoacyl-chitosan oligosaccharide.

Apparatus

Scanning electron micrograph (SEM) was characterized using S-4800 field emission scanning electron microscopy (Hitachi, Japan). Energy dispersive X-ray spectroscopy (EDS) was observed by a Zeiss Supra55 field emission scanning electron microscope (Zeiss, Germany). Ultraviolet absorption scanning was performed on a UV–vis spectrometer (TU-1901, PERSEE Analytics, Beijing, China). Infrared spectra absorption scanning was performed on a Fourier transform-infrared

spectrometer (Tensor 27, BRUKER, Billerica, MA, USA). Electrochemical data were obtained using a CHI660E electro-chemical workstation (Shanghai Chen Hua Co., China) connected to a three-electrode cell. The bare GCE (3 mm in diameter) or modified GCE, saturated calomel electrode, and platinum wire electrode were employed as the working, auxiliary, and reference electrodes, respectively.

Hardware and software

All computations were carried out on a computer with dual-core central processor and 2 GB of RAM. The quantum calculations were carried out using Gaussian 09 software.

Quantum chemical simulation

Some neutral amino acids were selected to fabricate 4-pentenoyl-aminoacyl-glucosamine (PAAGA) as the functional monomers. To estimate the preassembled system, especially the conjugation between BPA and functional monomer, charge transfer and binding energy were considered as main factors. In the course of a computer simulation, the structures of BPA and PAACO were optimized in the gas phase at the HF/6-31G(d) level of theory, and then the optimized geometry structures were verified without any imaginary frequency. The electronic stabilization energy, ΔE, was calculated by the following equation:

$$\Delta E = E(template - monomer\ complex) - E(template) - E(monomer)$$

All calculations were performed by using Gaussian 09 software.

Table S1 The chosen monomers and their computed energies in the absence and presence of BPA in gas phase.

Molecules	***E*** **(**Hartree**)**	**Δ*E*** **(**Hartree**)**	**Δ*E*** (kj/mol)[a]
BPA	-727.05296818	–	–
4-pentenyl-alanyl-glucosamine (PALAGA)	-1177.027281	–	–
4-pentenyl-asparaginyl-glucosamine (PASNGA)	-1344.827885	–	–
4-pentenyl-glutaminyl-glucosamine (PGLNGA)	-1383.865264	–	–
4-pentenyl-Glycinyl-glucosamine (PGLYGA)	-1137.998632	–	–
4-pentenyl-isoleucinyl-glucosamine (PILEGA)	-1294.125873	–	–
4-pentenyl-leucinyl-glucosamine (PLEUGA)	-1294.135435	–	–
4-pentenyl-methioninyl-glucosamine (PMETGA)	-1652.61039	–	–
4-pentenyl-phenylalanyl-glucosamine (PPHEGA)	-1406.60403	–	–
4-pentenyl-serinyl-glucosamine (PSERGA)	-1251.904866	–	–
4-pentenyl-threoninyl-glucosamine (PTHRGA)	-1290.93793	–	–
4-pentenyl-tyrosinyl-glucosamine (PTYRGA)	-1481.431211	–	–
4-pentenyl-valine-glucosamine (PVALGA)	-1255.113943	–	–
BPA- PALAGA	-1904.1164345	-0.03618632	-95.00718316
BPA- PASNGA	-2071.90458335	-0.02373021	-62.30366636
BPA- PGLNGA	-2110.93540088	-0.01716913	-45.07755082
BPA- PGLYGA	-1865.08003827	-0.02843761	-74.66294506
BPA- PILEGA	-2021.21670947	-0.03786804	**-99.42253902**
BPA- PLEUGA	-2021.2192291	-0.03082602	-80.93371551
BPA- PMETGA	-2379.69097059	-0.02761211	-72.4955948
BPA- PPHEGA	-2133.66363078	-0.0066322	-17.4128411
BPA- PSERGA	-1978.9665389	1978.957834	-22.85505626
BPA- PTHRGA	-2018.00801801	-0.01712019	-44.94905885
BPA- PTYRGA	-2208.51890199	-0.03472272	-91.16450136
BPA- PVALGA	-1982.18433216	-0.01742122	-45.73941311

[a]: 1 Hartree = 2625.5 kj/mol.

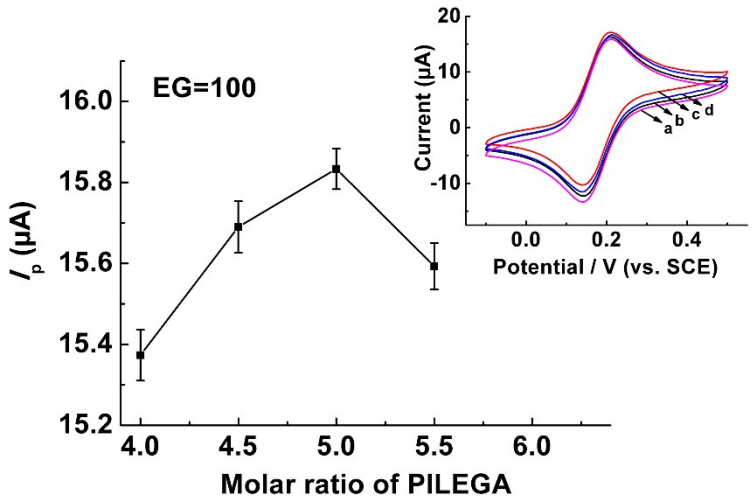

Fig. S1 Influence of the molar ratio of PICO to EGDMA on molecularly imprinted membrane permeability in 0.3 M NaAc/HAc (pH 6.5) solution containing 1.0 mM FEC. Inset: CV curves of membrane electrode prepared by different molar ratio of PICO to EGDMA, a: 4.0, b: 4.5, c: 5.0, d: 5.5. The molar ratio of EGDMA was fix at 100.

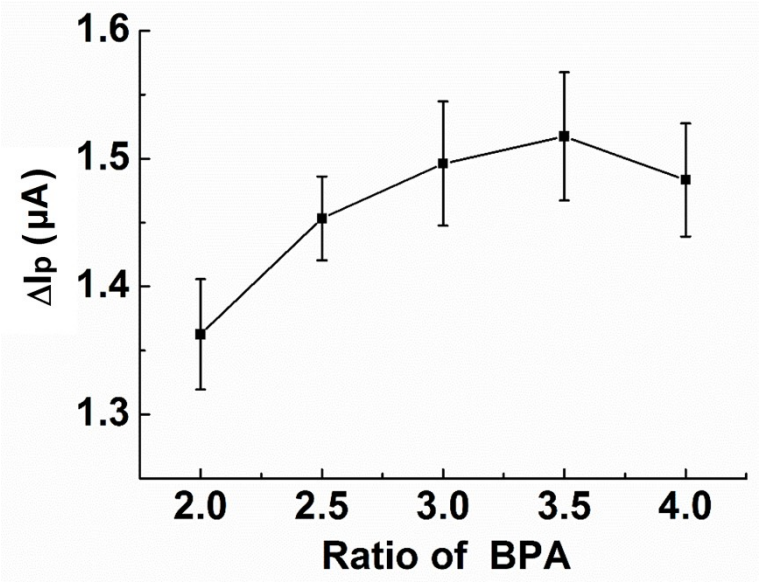

Fig. S2 Effect of the molar ratio of template, and monomer crosslinking agent added in the polymerization on the response of the sensor to 0.2 μM BPA in 0.3 M NaAc/HAc (pH 6.5) solution containing 1.0 mM ferrocenemethanol. The molar ratio of PILEGA to EGDMA was fixed at 5:100. The error bars represent the standard deviation of results (n=3).

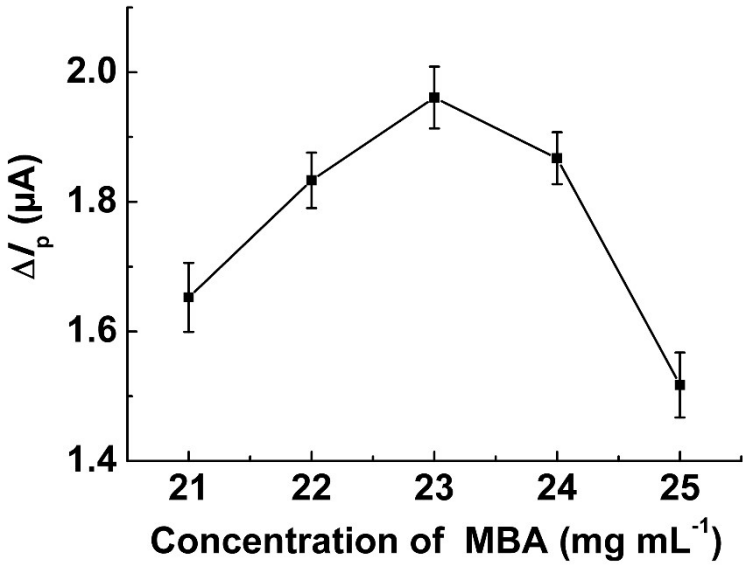

Fig. S3 Effect of the concentration of MBA in the second polymerization on the response of the sensor to 0.2μM BPA in 0.3 M NaAc/HAc (pH 6.5) solution containing 1.0 mM ferrocenemethanol. The error bars represent the standard deviation of results (n=3).

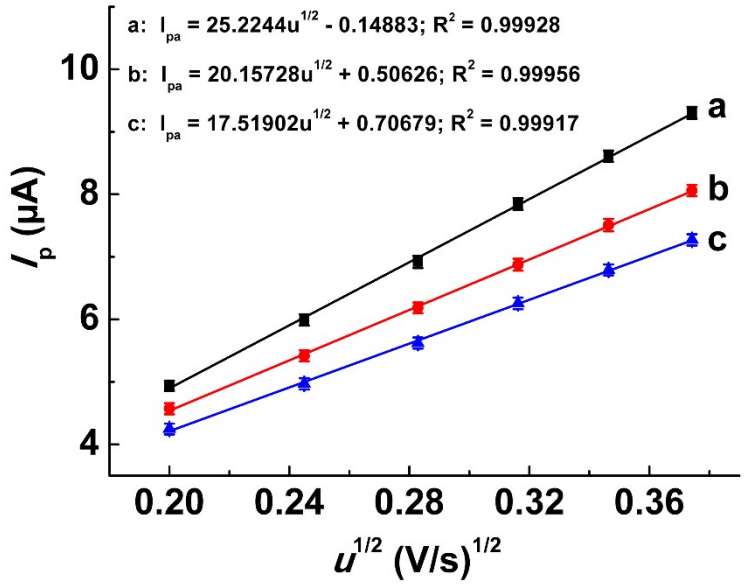

Fig. S4 Relationship between peak current of cyclic voltammetry vs square root of scan rate of polymeric film electrode in 0.3 M NaAc/HAc (pH 6.5) solution containing 1.0 mM ferrocenemethanol, at MBA concentrations: a) 11 mg mL^{-1}, b) 11.5 mg mL^{-1}, c) 12 mg mL^{-1}. The error bars represent the standard deviation of results (n=3).

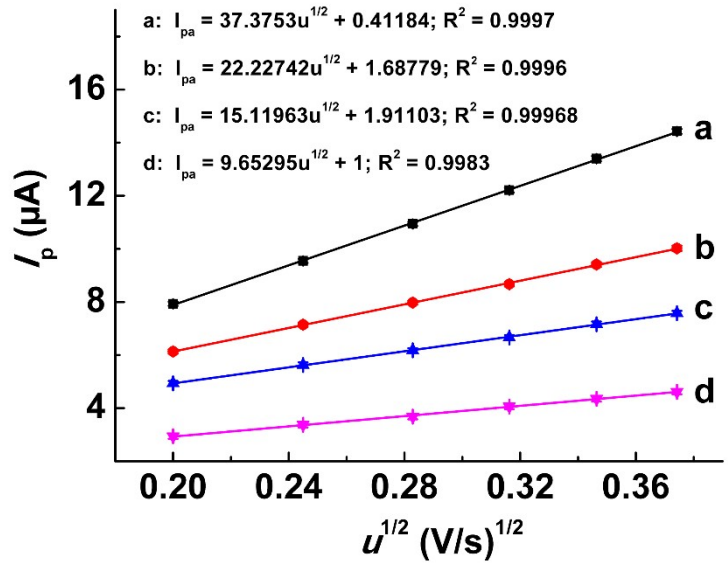

Fig. S5 Relationship between peak current of cyclic voltammetry vs square root of scan rate of polymeric film electrode in 0.3 M NaAc/HAc (pH 6.5) solution containing 1.0 mM ferrocenemethanol, at BPA concentrations: a) 0.5 mg mL^{-1}, b) 0.2 mg mL^{-1}, c) 0.1 mg mL^{-1}, d) 0 mg mL^{-1}; MBA concentrations: 13 mg mL^{-1}. The error bars represent the standard deviation of results (n=3).

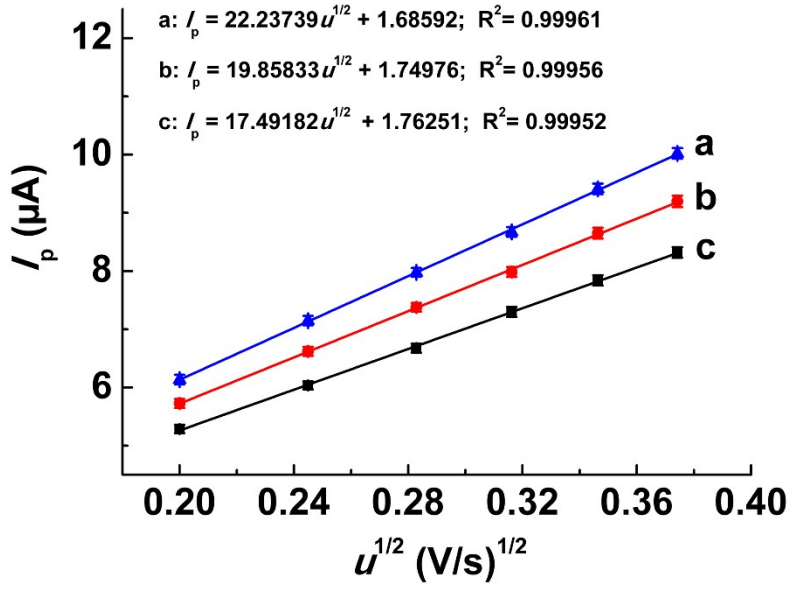

Fig. S6 Relationship between peak current of cyclic voltammetry vs square root of scan rate of polymeric film electrode in 0.3 M NaAc/HAc (pH 6.5) solution containing 1.0 mM ferrocenemethanol, at different mole rate of AA/BPA, a) 4:1, b) 3.75:1, c) 3.5:1; MBA concentrations: 13 mg mL^{-1}; BPA concentrations: 0.1 mg mL^{-1}. The error bars represent the standard deviation of results (n=3).

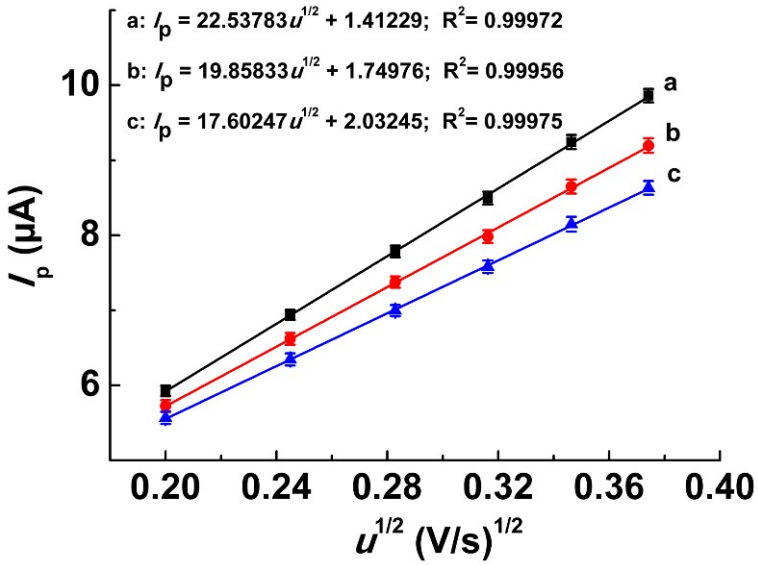

Fig. S7 Relationship between peak current of cyclic voltammetry vs square root of scan rate of Secondary imprinted film electrode prepared at different scanning cycles: a) 5, b) 6, c) 7 in 0.3 M NaAc/HAc (pH 6.5) solution containing 1.0 mM ferrocenemethanol; MBA concentrations: 13 mg mL^{-1}; BPA concentrations: 0.1 mg mL^{-1}, AA/MBA=3.75:1. The error bars represent the standard deviation of results (n=3).

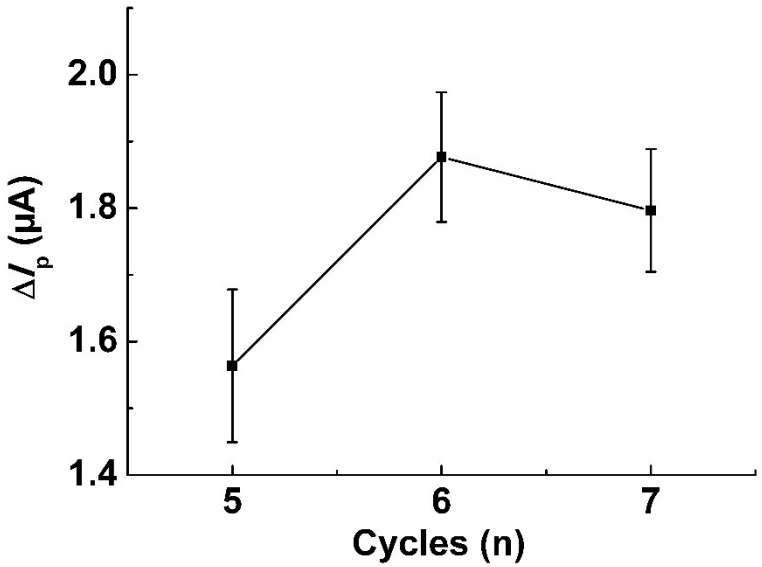

Fig. S8 The DPV response of electrochemical sensor toward 1.0 μM BPA prepared by different CV scanning cycles in 0.3 M NaAc/HAc (pH 6.5) solution containing 1.0 mM ferrocenemethanol. The error bars represent the standard deviation of results (n=3).

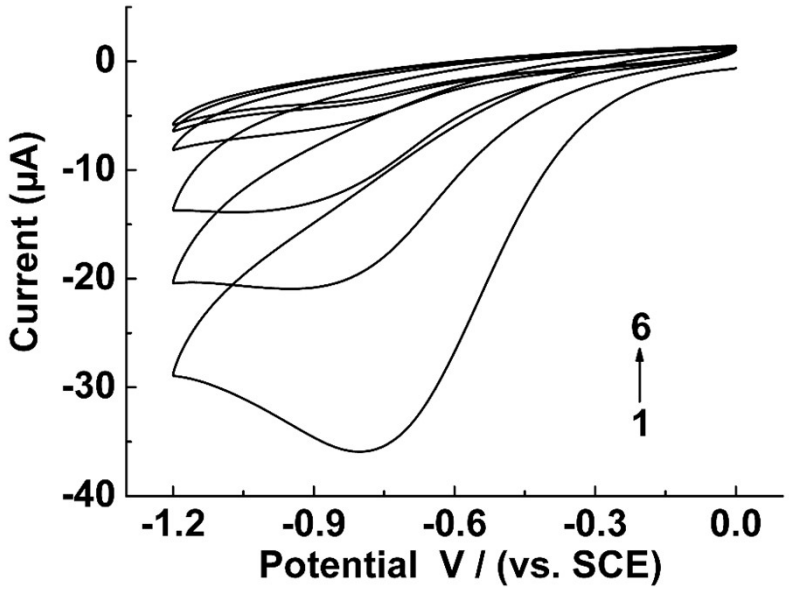

Fig. S9 Cyclic voltammograms for the electrochemical polymerization of MBA (13 mg mL^{-1}), AA (0.117 mg mL^{-1}), BPA (0.1 mg mL^{-1}), initiated by APS (1.25 mg mL^{-1}) in 0.3 M NaAc/HAc (pH 6.5) solution containing 1.0 mM ferrocenemethanol. Scan rate: 20 mV s^{-1}.

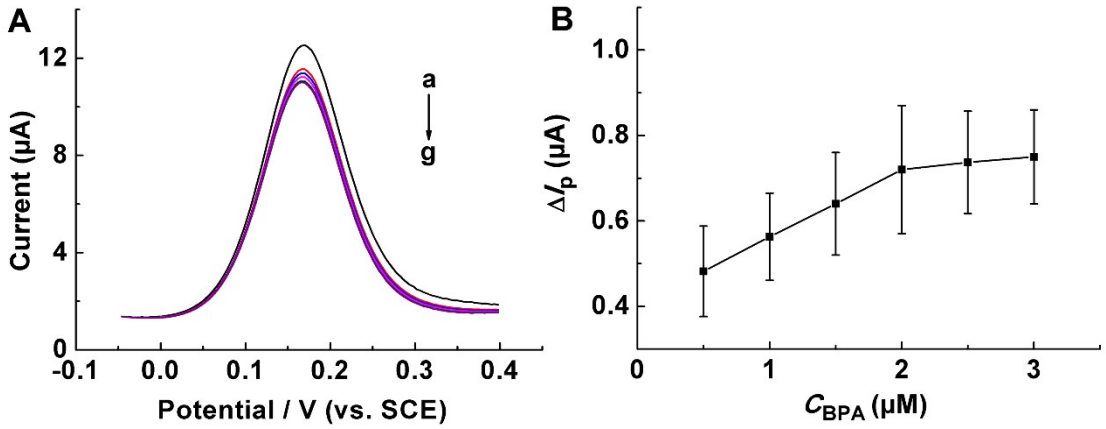

Fig. S10 (A) DPV of NIM(MIPs)/MWCNTs/GCE in 0.3 M NaAc/HAc solution (pH 6.5) containing 1.0 mM FCM at different BPA concentrations, a: 0 μM, b: 0.5 μM, c: 1.0 μM, d: 1.5 μM, e: 2.0 μM, f: 2.5 μM, g: 3.0 μM. (B) The corresponding calibration curve. Error bars represent the standard deviation of results (n=3).

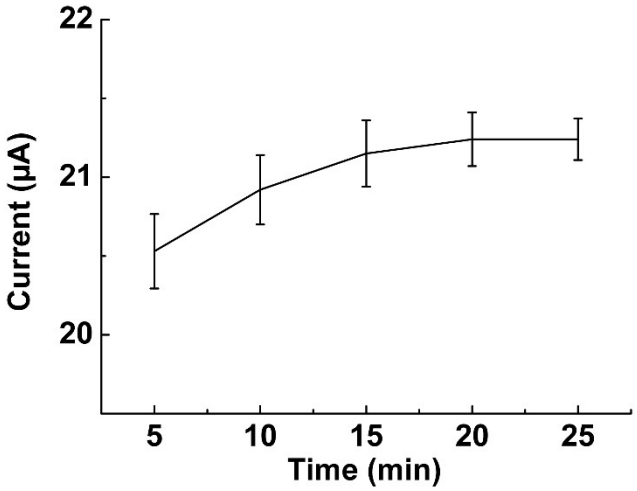

Fig. S11 DPV response of the prepared MIM(MIPs)/MWCNTs/GCE after desorption in methanol/acetic acid (3:1, v/v) solution for different time. Error bars represent the standard deviation of results (n=3).

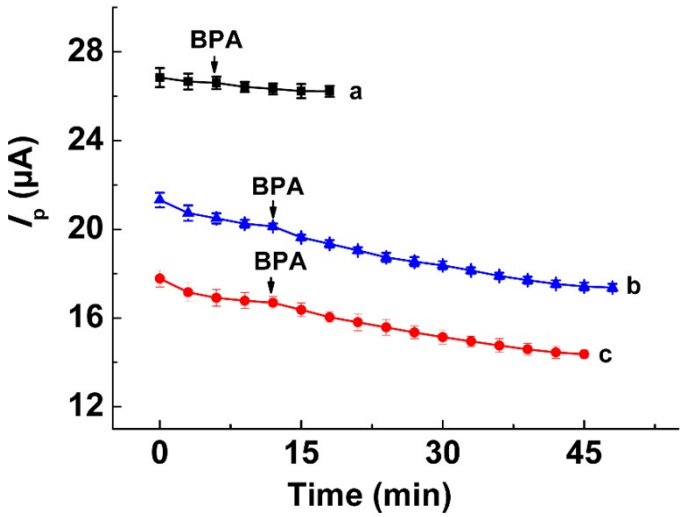

Fig. S12 Effect of incubation time on the current response of different modified electrodes recorded in 0.3 M NaAc/HAc (pH 6.5) solution containing 1.0 mM ferrocenemethanol and 2 μM BPA every 3 mins: a) BPA-MIM/MWCNTs/GCE; b) BPA-MIM(MIPs)/MWCNTs/GCE; c) BPA-MIM(MIPs)/GCE. Arrows in the chart indicate when BPA was added. The error bars represent the standard deviation of results (n=3).

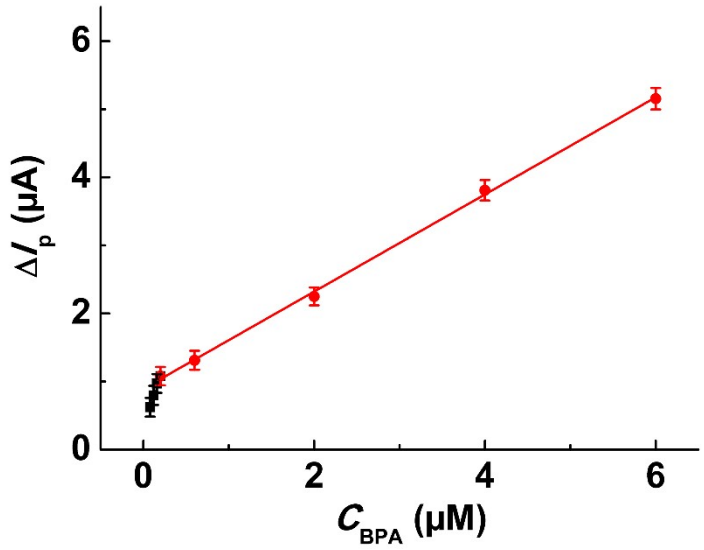

Fig. S13 The calibration curve for BPA-MIM(MIPs)/GCE electrode in 0.3 M NaAc/HAc (pH 6.5) solution containing 1.0 mM ferrocenemethanol. Error bars represent the standard deviation from 3 parallel tests.

Table S2 Comparison of different sensors of BPA.

Electrode configuration	Methods	Linear range (μM)	LOD (nM)	References
MWCNT/AuNP/Paper	LSV	0.876–87.6	131	1
AuPdNP/GrN/GCE	DPV	0.05–10.0	8	2
MIP/CNTs-Au NPs/BOMC/GCE	DPV	0.01–10.0	5	3
MIP/β-CD/RGO/GCE	DPV	0.02–1000.0	10	4
MIP/PPy@LSG	DPV	0.05–5.0	8	5
MIM(MIPs)/MWCNTs/GCE	DPV	0.04–8.0	8	Present work

Abbreviations: LSV–Linear Sweep Voltammetry; DPV–Differential Pulse Voltammetry; CV–Cyclic Voltammetry; GCE–Glassy Carbon Electrode; SPE–Screen Printed Electrode; AuPdNP–Gold Paladium Nanoparticles; GrN–Graphene Nanosheets; MWCNT–Multiwalled Carbon Nanotubes; β-CD–β-cyclodextrin; RGO- Reduced Graphene Oxide; PPy–Polypyrrole; LSG–Laser Scribed Grapheme.

References

[1] H. Y. Li, W. Wang, Q. Lv, G. C. Xi, H. Bai and Q. Zhang, *Electrochem. Commun*., 2016, **68**, 104–107.

[2] B. Y. Su, H. L. Shao, N. Li, X. M. Chen, Z. X. Cai and X. Chen, *Talanta*, 2017, **166**, 126–132.

[3] X. P. Hu, Y. Y. Feng, H. Wang, F. Q. Zhao and B. Z. Zeng, *Anal. Methods*, 2018, **10**, 4543–4548.

[4] H. Ali, S. Mukhopadhyay and N. R. Jana, *New J. Chem*., 2019, **43**, 1536–1543.

[5] T. Beduk, A. A. Lahcen, N. Tashkandi and K. N. Salama, *Sensors Actuators B: Chem*., 2020, **314**, 128026.